WILEY-VCH

FULL PAPER

Novel Pyridine-Based Hydroxamates and 2'-Aminoanilides as Histone Deacetylase Inhibitors: Biochemical Profile and Anticancer Activity

Clemens Zwergel[+],[a] Elisabetta Di Bello[+],[a] Rossella Fioravanti,[a] Mariarosaria Conte,[b] Angela Nebbioso, [b] Roberta Mazzone,[a] Gerald Brosch,[c] Ciro Mercurio,[d] Mario Varasi,[d] Lucia Altucci,[b] Sergio Valente,*[a] and Antonello Mai[a]

[a] Dr. C. Zwergel, Dr. E. Di Bello, Dr. R. Fioravanti, Dr. R. Mazzone, Prof. S. Valente, Prof. A. Mai
Department of Drug Chemistry and Technologies, Sapienza University of Rome, P. le A. Moro 500185 Rome (Italy)
E-mail: sergio.valente@uniroma1.it.

[b] Dr. M. Conte, Prof. A. Nebbioso, Prof. L. Altucci
Department of Precision Medicine, Università degli Studi della Campania Luigi Vanvitelli, Vico L. De Crecchio, 7-80138, Naples (Italy)

[c] Prof. G. Brosch
Institute of Molecular Biology, Biocenter, Medical University of Innsbruck, 6020 Innsbruck, Austria.

[d] Dr. M. Varasi, Dr. C. Mercurio
Department of Experimental Oncology, Academic Drug Discovery, European Institute of Oncology IRCCS, Via Adamello 16, 20139 Milan, Italy

[+] These authors contributed equally to this work

Supporting information for this article is given via a link at the end of the document.

Abstract: Starting from the *N*-hydroxy-3-(4-(2-phenylbutanoyl)amino)phenyl)acrylamide **5b** previously described by us as HDAC inhibitor, we prepared four aza-analogues of **5b** (**6-8, 9b**) as regioisomers containing the pyridine nucleus. A preliminary screening against mHDAC1 highlighted the *N*-hydroxy-5-(2-(2-phenylbutanoyl)amino)pyridyl)acrylamide **9b** as the most potent inhibitor. Thus, we further developed both pyridylacrylic- and nicotinic-based hydroxamates (**9a, 9c-f,** and **11a-f**) and 2'-aminoanilides (**10a-f** and **12a-f**), related to **9b**, to be tested against HDACs. Among them, the nicotinic hydroxamate **11d** displayed subnanomolar potency (IC_{50}: 0.5 nM) and selectivity up to 34000-fold over HDAC4 and from 100- to 1300-fold over all the other tested HDAC isoforms. The 2'-aminoanilides were class I-selective HDAC inhibitors, generally more potent against HDAC3, with the nicotinic anilide **12d** being the most effective (IC_{50}^{HDAC3} = 0.113 μM). When tested in U937 leukemia cells, the hydroxamates **9e**, **11c**, and **11d** blocked over 80% cells in G2/M phase, whereas the anilides did not alter the cell cycle progress. In the same cell line, the hydroxamate **11c** and the anilide **10b** induced about 30% apoptosis, and the anilide **12c** displayed about 40% cytodifferentiation. Finally, the most potent compounds in leukemia cells **9b**, **11c**, **10b**, **10e**, and **12c** were also tested in K562, HCT116, and A549 cancer cells, displaying antiproliferative IC_{50} values at single-digit to sub-micromolar level.

Introduction

In eukaryotic biological processes, epigenetic alterations resulting in the gain or loss of function of regulatory proteins contribute fundamentally to human diseases' onset and progression [1]. One of the most studied epigenetic targets in the last three decades are histone deacetylases (HDACs) [2].

Human HDACs have been investigated as key components of the epigenetic machinery regulating gene expression and often behave as oncogenes in cancer except for HDAC2 [3]. Besides HDAC deregulation and/or overexpression in cancer, these enzymes are also involved in neurological diseases, inflammation, parasite infections, and other human disorders [4].

HDAC inhibitors (HDACi) are capable to activate several antitumor pathways, such as extrinsic (death receptors and ligands upregulation) or intrinsic (downregulation of anti-apoptotic factors, upregulation of pro-apoptotic ones) apoptosis induction. Furthermore, HDACi either target directly or modulate indirectly the (over)expression of non-histone proteins. They influence a whole bunch of inflammation/immune response mediators, transcription factors and regulators, chaperones, and structural proteins as well as DNA repair enzymes [2-3, 5]. These enzymes can also induce senescence, growth arrest via p21 upregulation or downregulation of cyclins, lead to mitotic and autophagic cell death, and possess anti-angiogenic effects via HIF-1α function or VEGF downregulation [6].

A large number of HDACi are involved in preclinical as well as clinical settings [6c, 7]. HDACi are mainly used in blood cancers such as leukemias and are poorly successful in solid tumors as single agents [8]. Inhibitors designed for HDACs have in common a well-validated pharmacophore model composed of a zinc-binding group (ZBG) attached to a linker chain (hydrophobic spacer, HS) mimicking the lysine side chain terminated by a functional "cap" group. A connecting unit (CU) between the cap and the linker chain can also be modulated to improve interactions [6c].

In detail, most HDACi typically possess either an hydroxamate or a 2-aminoanilide function as ZBG. Numerous examples are described in the recent literature and have been summarized in various reviews [2, 4c, 6c].

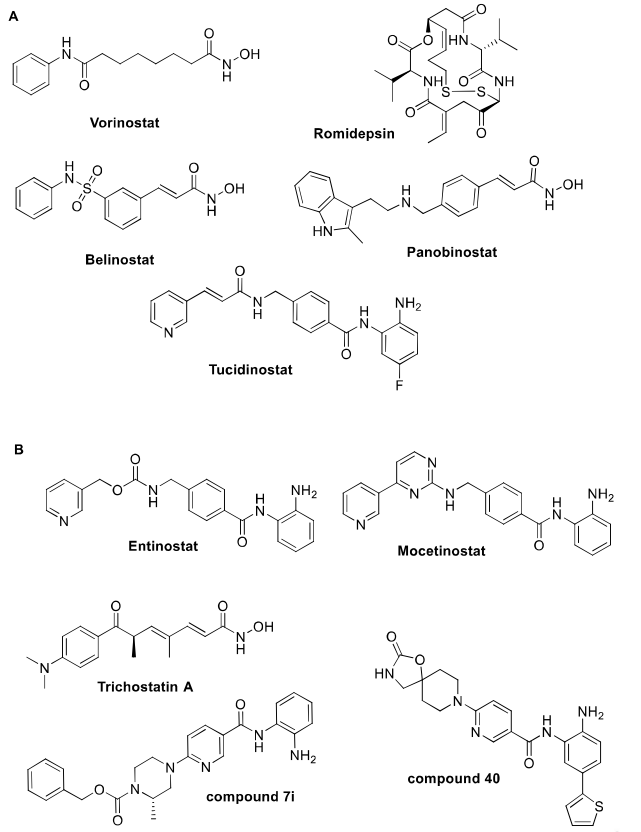

Figure 1. (**A)** Chemical structures of HDAC inhibitors approved by FDA and CFDA. (**B**) Chemical structures of HDAC inhibitors in clinical trials and active in preclinical settings

So far, only five HDACi have reached the market: the pan-HDAC inhibitor vorinostat (SAHA) [9] and the HDAC1,2 selective inhibitor romidepsin (FK-228) [10] were both approved for the treatment of refractory cutaneous T-cell-lymphoma (CTCL), and the latter also for peripheral T-cell lymphoma (PTCL); moreover, the pan-HDAC inhibitors belinostat (PDX101) and panobinostat (LBH589) [11] have been applied for the treatment of PTCL and [12] multiple myeloma (MM), respectively. All drugs mentioned above have been approved by the FDA, whereas tucidinostat (chidamide), active against HDAC1, -2, -3, -10 was approved for PTCL only in China in 2015 [6c] (Figure 1A).

Entinostat (MS-275) (Figure 1B) is a HDAC1-3 selective inhibitor in clinical trials that can be used alone or in combination with 5-azacytidine or ganciclovir for the treatment of myelodysplastic syndrome (MDS), chronic myeloid leukemia (CML), acute myelogenous leukemia (AML) and cancer-related viral infections such as Epstein-Barr virus (EBV) [13]. Mocetinostat, a HDAC1,2 selective inhibitor, is currently evaluated in numerous cancer types, especially in leukemia and lymphoma. Trichostatin A (TSA), a pan-HDAC inhibitor, is currently evaluated in many types of diseases, including pancreatic adenocarcinoma, HIV infection, CML, BCR/ABL positive breast cancer [14] (Figure 1B). In 2007, Hamblett *et al*. explored around the nicotinamide core, describing several compounds displaying good selectivity against HDAC1 and high capability to induce cell cycle arrest, apoptosis, and cytodifferentiation in human leukemia U937 cells. Furthermore, extensive exploration around of these compounds led to the discovery of the class I selective HDACi **7i** and compound **40** (Figure 1B) with a good *in vivo* efficacy in a HCT116 xenograft model [15].

Our research group acquired extensive experience in the design of HDACi in the last two decades [6c, 13, 16]. In 2001, we described a new class of selective HDACi, 3-(4-aroyl-1*H*-2-pyrrolyl)-*N*-hydroxy-2-propenamides (APHAs, **1**, Figure 2) as agents capable of inhibiting HDAC activity in the micromolar range, characterized by an aroyl moiety as CAP+CU, a pyrrylacrylic moiety as HS, and the hydroxamate group as ZBG [16e, 16g, 17]. Extensive structure-activity relationship studies performed on the **1** model led to analogues with improved HDAC inhibitory potency and good anticancer properties in mouse A20 cells[16a].

Later, through a structure-based drug design, two isomers of the APHA scaffold, the 3-(2-aroyl-1-methyl-1*H*-pyrrol-4-yl)-*N*-hydroxy-2-propenamide and the 3-(2-aroyl-1-methyl-1*H*-pyrrol-5-yl)-*N*-hydroxy-2-propenamide (*iso*-APHAs **2**, Figure 2), were designed and prepared. When tested in human leukemia U937 cell line, the (*E*)-3-(5-([1,1'-biphenyl]-4-carbonyl)-1-methyl-1*H*-pyrrol-3-yl)-*N*-hydroxy-2-propenamide impaired cell cycle while inducing apoptosis and cytodifferentiation [16e]. A vinylogy study applied on the **2** model allowed us to discover a new series of compounds, the (aryloxopropenyl)pyrrolyl hydroxyamides (**3**), as selective inhibitors of class II HDACs. The hit compound, MC1568 (Ar_2 = 3-fluorophenyl, Figure 2), has been extensively used as a tool for dissecting the HDAC biological functions in different cell contexts, including cancers, type 2 diabetes, hepatic and renal fibrosis, amyotrophic lateral sclerosis (ALS), influenza A virus and HIV [16j, 16l, 18].

Replacement of the pyrrole with benzene or pyridine ring in the scaffold **3** afforded the *N*-hydroxy-3-(4-(3-oxo-3-phenylprop-1enyl)phenyl/pyridin)acrylamides (**4**) (Figure 2) [16i, 16j], acting as anticancer agents through HDAC inhibition. A further change of the oxopropenyl with an amide moiety led to the *N*-hydroxy-3-(acylaminophenyl)acrylamides (**5**) (Figure 2) [16c] as an additional class of HDACi potent up to nanomolar level [16c]. Most of the tested compounds showed a preference for HDAC1 inhibition and were able to arrest the U937 cell cycle in the G2/M phase [16h].

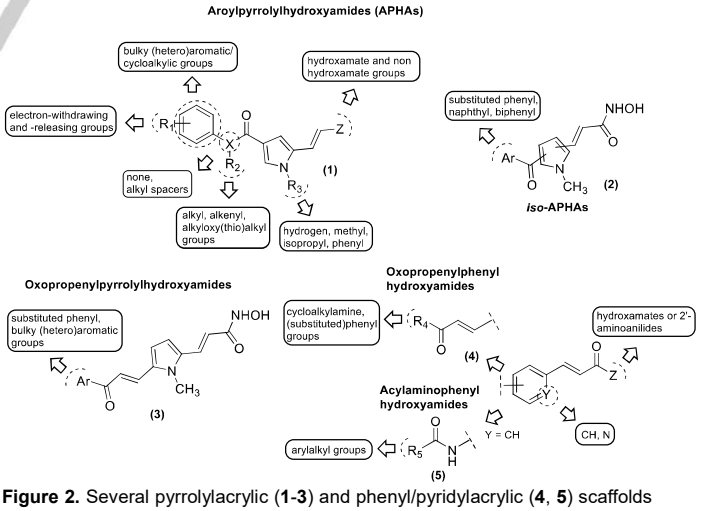

Figure 2. Several pyrrolylacrylic (**1**-**3**) and phenyl/pyridylacrylic (**4**, **5**) scaffolds developed by our research group for HDACi design.

Results and Discussion

Following our previous investigations mentioned above [16b, 16h-j], and taking into account that pyridine-based HDACi were active in preclinical settings [15], we selected the *N*-(4-(3-(hydroxyamino)-3-

oxoprop-1-en-1-yl)phenyl)-2-phenylbutanamide **5b** as one of the most potent compounds among the **5** series, and designed and prepared four corresponding pyridine-based regioisomers, **6-8** and **9b**, to be tested against mouse HDAC1 (mHDAC1). The results clearly highlighted that the *N*-(5-(3-(hydroxyamino)-3-oxoprop-1-en-1-yl)pyridin-2-yl)-2-phenylbutanamide **9b** displayed the highest mHDAC1 inhibition (IC_{50}: 0.075 μM), being 4-fold more potent than the reference **5b**. Hence, we selected **9b** for further structural optimization. Two series of 2-acylamino-5-(3-oxoprop-1-en-1-yl)pyridine hydroxamates (**9a**,**c-f**) and 2'-aminoanilides (**10a-f**), as well as the corresponding nicotinic analogs **11a-f** (hydroxamates) and **12a-f** (2'-aminoanilides), were designed and synthesized to be tested in enzyme and in cellular assays. At the acyl moiety, the derivatives differ in the presence of phenylacetyl groups with growing substituents at the methylene unit (ethyl, *iso*-propyl, benzyl), or of the bulkier 1- and 2-naphthylacetyl groups (Figure 3).

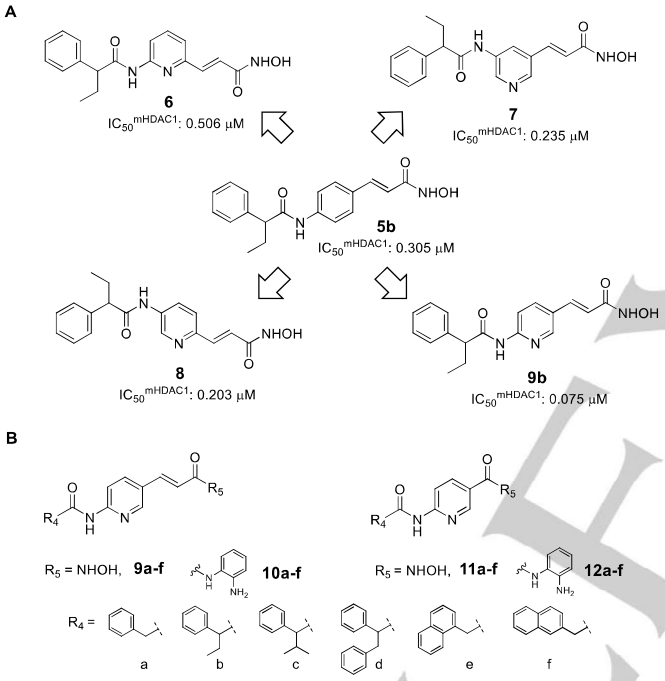

Figure 3. Design of (A) novel pyridine hydroxamates isomers **6-8** and **9b**, and (B) 2-acylamino-5-(3-oxoprop-1-en-1-yl)pyridine hydroxamates **9a-f** and 2'-aminoanilides **10a-f**, as well as the corresponding nicotinic analogs **11a-f** (hydroxamates) and **12a-f** (2'-aminoanilides).

Synthetic routes of novel pyridine-based hydroxamates **6-8**, **9a-f**, and **11a-f,** and 2'-aminoanilides **10a-f** and **12a-f**.

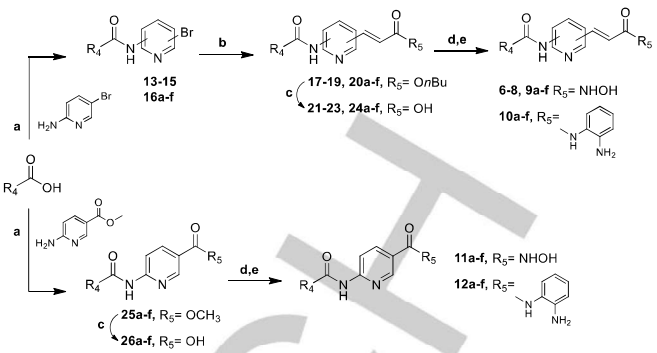

Scheme 1. Reagents and conditions: a) i) $SOCl_2$, 80°C; ii) Et_3N, CH_2Cl_2; b): *Method 1*: $Pd(OAc)_2$, Et_3N , *n*-butyl acrylate, anhydrous DMA, 100° C, sealed tube, 8h; *Method 2*. $P(Ph)_3$, $Pd(OAc)_2$, Et_3N , *n*-butyl acrylate, $NaHCO_3$, anhydrous DMF, 100° C, sealed tube, 2h; *Method 3:* $P(Ph)_3$, $Pd(OAc)_2$, *n*-BuN_4I, NaOAc x 3 H_2O, H_2O, butyl acrylate, 140° C, anhydrous DMF, overnight; c) KOH o LiOH, H_2O, EtOH; **d)** i) $ClCOOC_2H_5$, Et_3N, THF, 0° C; ii) $NH_2OC(CH_3)_2OCH_3$; iii) Amberlist 15, CH_3OH; **e)** Et_3N, BOP reagent, 1,2-phenylendiamine, DMF, N_2.

For the synthesis of the lead compounds, the appropriate commercial carboxylic acids were treated with thionyl chloride and then with 2-amino-5-bromopyridine, or with methyl 6-aminonicotinate, in the presence of triethylamine to afford the amides **13-15** and **16a-f** or **25a-f**, respectively. The bromopyridylamides **13-15** and **16a-f** underwent Heck reaction (three different methods) to obtain the pyridylacrylate intermediates **17-19** and **20a-f**. The esters **17-19**, **20a-f**, and **25a-f** were hydrolyzed in basic medium to the corresponding carboxylic acids **21-23**, **24a-f**, and **26a-f**, respectively. Next, these compounds were activated with ethyl chloroformate and triethylamine, and subsequently treated with *O*-(2-methoxy-2-propyl)hydroxylamine and then Amberlyst 15 ion-exchange resin in methanol to yield the hydroxamates **6-8**, **9a-f**, and **11a-f**. Alternative treatment of the acids **24a-f** and **26a-f** with benzotriazole-1-yloxytris(dimethylamino)-phosphonium hexafluorophosphate (BOP reagent), triethylamine and 1,2-phenylenediamine afforded the corresponding 2'-aminoanilides **10a-f** and **12a-f**, respectively (Scheme 1). Chemical and physical data of the final compounds **6-12** and the intermediates **13-26** as well as elemental analyses for the final compounds are reported in tables S1**–**S10 in Supporting Information.

Biochemical activities of 9a-f, 11a-f, 10a-f, and 12a-f against human recombinant (hr) HDAC isoforms

The new hydroxamates **9a-f**, **11a-f,** and 2-aminoanilides **10a-f**, **12a-f** were screened in 10-dose IC_{50} mode with 3-fold serial dilution starting from 100 μM solutions, against selected hrHDAC1, -3, -4, -6, and -8, representatives of class I (HDAC1,3,8), class IIa (HDAC4) and class IIb (HDAC6) HDACs, to assess their inhibitory capability. For this purpose, either the fluorogenic peptide from p53 residues 379-382 (RHKK(Ac)AMC) substrate (for HDAC1, -3, -6), or the fluorogenic class IIa (Boc-Lys(trifluoroacetyl)-AMC) substrate (for HDAC4), or the diacetylated peptide from p53 residues 379-382 (RHK(Ac)K(Ac)AMC) substrate (for HDAC8) has been used, and SAHA was employed as reference compound and positive control.

The biochemical data (Table 1) highlighted that both the pyridylacrylic (**9a-f**) and the nicotinic (**11a-f**) hydroxamates potently and selectively inhibited HDAC6. In detail, the first group showed IC_{50} values ranging from submicromolar (**9a**, IC_{50}= 164

nM) to single-digit nanomolar (**9e**, IC_{50}: 7 nM) level. In particular, **9e**, bearing the 1-naphthylacetyl moiety at the amide function, displayed up to 1000-fold selectivity for HDAC6 over HDAC4 and more than 38- or 50-fold selectivity over all the other tested HDAC isoforms. The nicotinic hydroxamates **11a-f** were even more potent against HDAC6 than **9a-f**, reaching subnanomolar inhibition with **11d** (IC_{50}^{HDAC6} = 0.5 nM), characterized by a 2,3-diphenylpropanamide moiety at the pyridine C2 position, whereas all the other analogs (**11a-c**,**e-f**) provided dual- to single-digit nanomolar inhibition. Noteworthy, the nicotinic series displayed very high selectivity for HDAC6: indeed, **11d** displayed up to 34000-fold selectivity over HDAC4 and from 100- to 1300-fold over all other HDAC isoforms. Moreover, in both pyridylacrylic and nicotinic hydroxamates, the insertion of a bulky or branched arylacetamide group at the pyridine C2 position increases the inhibition potency and selectivity towards HDAC6, when compared to the phenylacetyl derivatives **9a** and **11a**.

Regarding the 2'-aminoanilide series **10a-f** and **12a-f**, both the pyridylacrylic and nicotinic derivatives displayed, as predictable, HDAC1 and -3 selectivity, with a preference for HDAC3 over HDAC1. More in detail, both series displayed single-digit micromolar to submicromolar inhibition potency against HDAC1 and -3, with **10e** among the pyridylacrylic anilides, bearing the 1-naphthylacetamide moiety at C2, and **12d** among the nicotinic anilides, carrying a 3-methyl-2-phenylbutanamide portion at C2, being the most potent against HDAC3 (IC_{50} values: 0.187 and 0.113 μM, respectively).

Cell-cycle analyses, apoptosis induction and granulocytic differentiation in human U937 leukemia cells

Using FACS analysis, compounds **9a-f**, **10a-f**, **11a-f**, and **12a-f** were tested at 5 μM for 30 h in human U937 acute myeloid leukemia cell line to evaluate their effects on cell cycle, apoptosis, and granulocytic differentiation. SAHA and MS-275 were used as reference and positive controls. In cell cycle assays (Figure 4A), the nicotinic hydroxamates led to an arrest in G2/M phase (see **11c** and **11d**, 50% and 80% blockage, respectively), while the pyridinacrylic hydroxamates displayed a blockage of the cell cycle either at the S phase, with **9c** resulting in more than 60% blockage, or G2/M phase, with **9b**, **9d**, **9e**, the latter two being the most potent with about 80% blockage.

Table 1. Biochemical inhibition (IC_{50}, μM) of **9a-f**, **10a-f**, **11a-f** and **12a-f** towards hrHDAC 1, -3, -4, -6 and -8 isoforms. The HDAC6- (for **9**, **11**) or HDAC3- (for **10**, **12**) selectivity index is given in round brackets.

compound	HDAC1	HDAC3	HDAC4	HDAC6	HDAC8
9a	7.08 *(43.2)*	6.30 *(38.4)*	155 *(945)*	0.164	2.94 *(17.9)*
9b	1.56 *(130)*	1.23 *(102)*	31.7 *(2642)*	0.012	1.15 *(95.8)*
9c	2.26 *(141)*	2.19 *(137)*	39.4 *(2462)*	0.016	1.45 *(90.6)*
9d	2.02 *(91.8)*	0.781 *(35.5)*	27.3 *(1241)*	0.022	1.41 *(64.1)*
9e	0.271 *(38.7)*	0.351 *(50.1)*	7.05 *(1007)*	0.007	0.352 *(50.3)*
9f	0.425 *(32.7)*	0.581 *(44.6)*	10.7 *(823)*	0.013	0.552 *(42.3)*
10a	5.89 *(28.6)*	0.206	NA[a]	NA	135 *(655)*
10b	3.43 *(8)*	0.426	NA	98.3 *(231)*	86.8 *(204)*
10c	5.77 *(8.5)*	0.681	NA	115.8 *(170)*	98.5 *(145)*
10d	3.18 *(7.8)*	0.406	NA	NA	181 *(446)*
10e	0.366 *(2)*	0.187	NA	NA	140 *(749)*
10f	2.57 *(3.7)*	0.694	NA	309 *(445)*	NA
11a	2.42 *(142)*	2.71 *(159)*	26.0 *(1529)*	0.017	0.386 *(22.7)*
11b	1.12 *(187)*	0.917 *(153)*	28.8 *(4800)*	0.006	0.277 *(46.2)*
11c	1.0 *(167)*	0.665 *(111)*	46.6 *(7767)*	0.006	0.357 *(59.5)*
11d	0.117 *(234)*	0.056 *(112)*	17.2 *(34400)*	0.0005	0.643 *(1286)*
11e	1.03 *(147)*	0.765 *(109)*	14.4 *(2057)*	0.007	0.40 *(57.1)*
11f	0.784 *(41.3)*	0.301 *(15.8)*	6.0 *(316)*	0.019	1.0 *(52.6)*
12a	1.41 *(7)*	0.202	NA	NA	NA
12b	1.13 *(6.4)*	0.176	NA	NA	103 *(585)*
12c	1.27 *(6.9)*	0.185	NA	NA	136 *(735)*
12d	0.379 *(3.3)*	0.113	NA	NA	NA
12e	1.42 *(3.6)*	0.389	NA	NA	78 *(200)*
12f	2.36 *(3.1)*	0.752	NA	NA	96 *(128)*
SAHA	0.26	0.35	0.49	0.03	0.24

[a] NA, not active, impossible to calculate the IC_{50} even by extrapolation.

In addition, **11c** was unique to induce over 30% of the pre-G1 fraction, indicating a cell death effect, more potent than SAHA (about 15% of pre-G1 phase) in these assay conditions. None of the tested hydroxamates **9** and **11** were able to induce cytodifferentiation, which was evaluated through the expression of the surface antigen CD11c marker in propidium iodide (PI)-negative cells.

Concerning the 2'-aminoanilides **10a-f** and **12a-f**, none of both series displayed cell cycle arrest/death induction, with the only exception of **10b**, giving almost 30% of cell death and being more potent than SAHA in this assay. Moreover, **10b**, **10e**, and **12c** provided the most potent cytodifferentiating effects (40% CD11c-positive/PI-negative cells with **12c**), although less effective than

MS-275 (about 70% CD11c$^-$positive/PI negative cells) in these assay conditions.

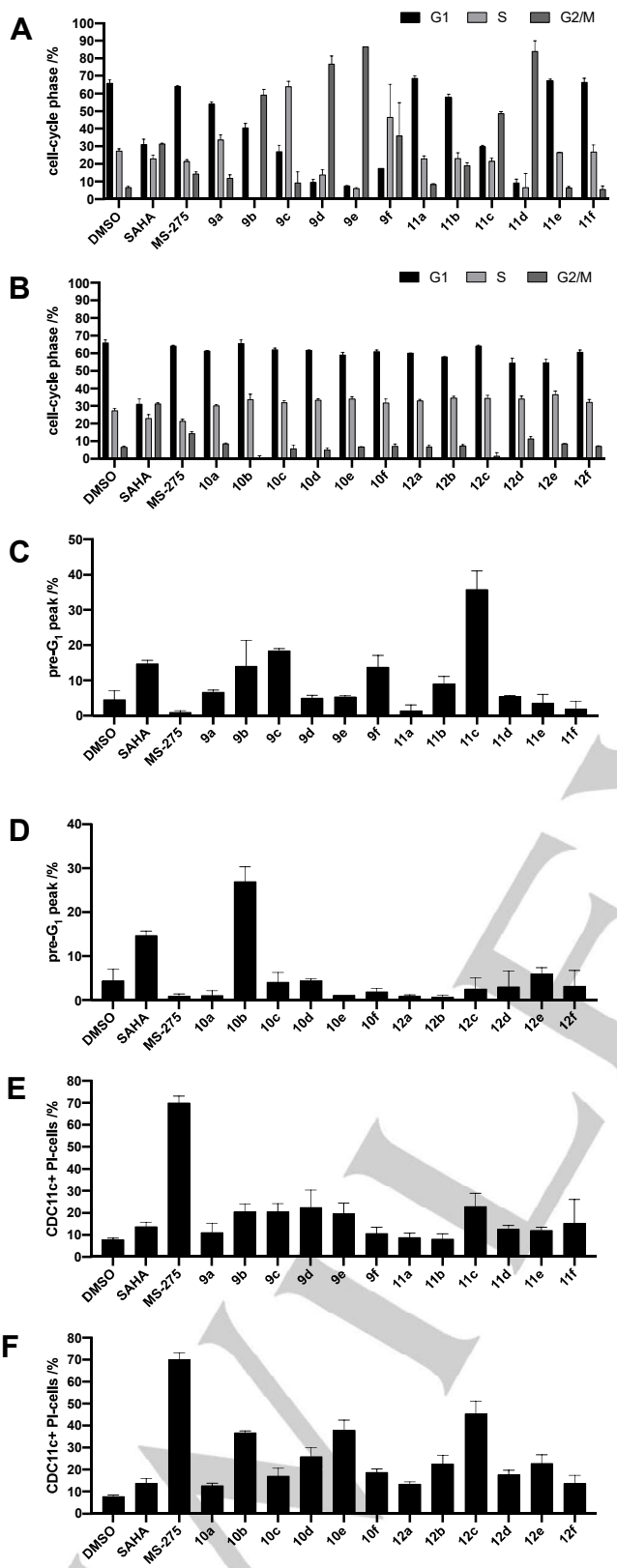

Figure 4. (A, B, C, D) Effects on cell cycle phases (E, F), and cytodifferentiation of hydroxamates **9a-f**, **11a-f,** and 2'-aminoanilides **10a-f**, **12a-f** in human U937 leukemia cells treated at 5 μM of compounds for 30 h.

Effects on acetylation level of histone (histone H3) and non-histone (α-tubulin) substrates

Next, to assess the in-cell target engagement, western blot analyses with specific antibodies were performed in human leukemia U937 cells to evaluate the effects on the acetylation levels of histone H3 and α-tubulin by the treatment with three of the most effective compounds **10e**, **11c,** and **12c**, tested at 5 μM for 24 h. SAHA and MS-275 were used as positive controls. As highlighted by Figure 5, the nicotinic hydroxamate **11c** confirmed to be a potent HDAC6 inhibitor since it induced a strong α-tubulin acetylation, even better than SAHA, whereas none of the nicotinic 2'-aminoanilides **10e** and **12c** provided any effect on acetyl-tubulin, as expected. In histone H3 acetylation assay, **10e**, **11c** and **12c** increased the acetyl-H3 level respect to the control, with **10e** and **11c** displaying a level comparable to those of SAHA and MS-275, tested in the same conditions.

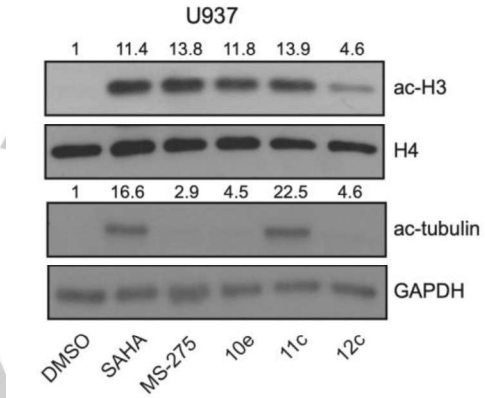

Figure 5. Effects on acetylation level of histone H3 (up) and a-tubulin (down) in U937 cells treated with the indicated compounds at 5 μM of compounds for 24 h. Histone H4 and GAPDH were used as loading controls.

According to the best profile proved in U937 leukemia cells, selected hydroxamates **9b**, **11c**, and the 2'-aminoanilides **10b**, **10e** and **12c** were screened against three different cancer cell lines, as human chronic myelogenous leukemia K562, colorectal carcinoma HCT116, lung adenocarcinoma A549, to assess their antiproliferative activities (IC_{50} values, Table 2). In general, both the hydroxamates and the 2'-aminoanilides displayed IC_{50} values ranging from single-digit to sub-micromolar levels against all the three tested cancer cell lines, with HCT116 and K562 being more responsive than A549 (Table 2) to the selected compounds treatment.

Table 2. Antiproliferative activity (IC_{50}, μM ± SD)[a,b] of selected compounds in a panel of human cancer cell lines

compound 1[a]	Colorectal carcinoma HCT116	Lung adenocarcinoma A549	Chronic myelogenous leukemia K562
9b	0.88 (±0.23)	2.67 (±0.12)	0.92 (±0.19)
11c	0.92 (±0.07)	2.06 (±0.14)	1.04 (±0.15)
10b	1.63 (±0.20)	5.72 (±0.86)	2.76 (±0.61)
10e	0.84 (±0.19)	4.26 (±1.11)	0.60 (±0.0007)
12c	3.15 (±0.09)	8.51 (±2.10)	3.11 (±0.64)

[a]Cells were treated for 72 h with various inhibitor concentrations; [b]Standard deviation (SD) is reported in round brackets.

Conclusion

In conclusion, in the present work we discuss first a regioisomeric study of novel acylaminopyridylacrylic hydroxamates **6-8** and **9b** as azaisosters of our previously reported cinnamyl hydroxamate **5b**. This preliminary screening led to the identification of the *N*-(5-(3-(hydroxyamino)-3-oxoprop-1-en-1-yl)pyridin-2-yl)-2-phenylbutanamide **9b** as the most potent HDAC inhibitor. By the following optimization of this scaffold, new **9b** analogs, both as pyridylacrylic and nicotinic hydroxamates **9a**, **9c-f**, and **11a-f**, and the corresponding 2'-aminoanilides **10a-f** and **12a-f** were designed and prepared. When tested against hrHDAC1, -3, -4, -6, and -8 isoforms, **9e** and **11d** proved to be most potent and selective against HDAC6 among the pyridylacrylic and nicotinic hydroxamates, respectively. In detail, **9e** displayed IC_{50} = 7 nM against HDAC6 and selectivity over the other HDAC isoforms ranging from 40- to 1000-fold, whereas **11d** displayed subnanomolar potency (IC_{50} = 0.5 nM) against HDAC6 and selectivity from 112- to 34000-fold over the other isoforms. The 2'-aminoanilides **10a-f** and **12a-f** preferentially inhibited class I HDACs, in particular HDAC3 with submicromolar potency. Among them, **10e** and **12d** were most potent against HDAC3, showing IC_{50} values of 0.187 and 0.113 μM, respectively. When tested in U937 leukemia cells to assess their capability to induce cell cycle arrest, apoptosis induction, and cytodifferentiation, the hydroxamates **9e**, **11c,** and **11d** blocked the cell cycle in G2/M phase (over 80% blockage), whereas the anilides did not alter cell cycle progression significantly. Among the tested compounds, the nicotinic hydroxamate **11c** and the pyridylacrylic 2'-aminoanilide **10b** were the sole to induce about 30% of proapoptotic effect. In cytodifferentiation assays, the hydroxamates had no effect, whereas the nicotinic 2'-aminoanilide **12c** exhibited about 40% of CD11c-positive/PI-negative cells.

Among the most effective compounds, the hydroxamate **11c** potently induced α-tubulin acetylation, proving HDAC6-engagement in U937, and both the 2'-aminoanilides **10e** and **12c** together with **11c** led to a strong histone H3 acetylation signal in the same cells.

The most efficient compounds in leukemia, i.e., **9b**, **11c**, **10b**, **10e**, and **12c,** were also screened against three further cancer cell lines, including K562 leukemia, HCT116 colon cancer, and A549 lung cancer cells, where they displayed antiproliferative activity at single-digit to sub-micromolar concentrations. Further studies are needed to assess the anticancer potential of such derivatives.

Experimental Section

Synthesis and characterization

General

Melting points were determined on a Büchi 530 melting point apparatus and are uncorrected. ^{1}H-NMR spectra were recorded at 400 MHz on a Bruker AC 400 spectrometer; chemical shifts are reported in δ (ppm) units relative to the internal reference tetramethylsilane (Me4Si). All compounds were routinely checked by TLC and 1H-NMR. TLC was performed on aluminum-backed silica gel plates (Merck DC, Alufolien Kieselgel 60 F254) with spots visualized by UV light. All solvents were reagent grade and, when necessary, were purified and dried by standard methods. Concentration of solutions after reactions and extractions involved using a rotary evaporator operating at reduced pressure of ca. 20 Torr. Organic solutions were dried over anhydrous sodium sulfate. Elemental analysis has been used to determine the purity of the described unknown final compounds, which is >95%. Analytical results are within ±0.40% of the theoretical values (Table S1 in Supporting Information). All chemicals were purchased from Sigma Aldrich s.r.l, Milan (Italy), or TCI Europe N.V., Zwijndrecht (Belgium), and were of the highest purity.

General procedure for the synthesis of nicotinates 13-15, 16a-f, and 25a-f. Example: methyl 6-(3-methyl-2-phenylbutanamido)nicotinate (25c).

3-methyl-2-phenyl-butyryl chloride (6.1 mmol, 1.0 g) and triethylamine were added to a solution of 6-amino-methylnicotinate (6.1 mmol, 1.39 g) in DCM dry (20 mL) at 0 °C. After stirring at room temperature for two hours, the reaction was quenched with water (50 mL) and extracted with dichloromethane (3 x 50 mL). The organic phase was then washed with brine (100 mL), dried over sodium sulfate, and evaporated under reduced pressure. The residual crude was finally purified by column chromatography on silica gel eluting with a mixture ethyl acetate:*n*-hexane 1:5.

Mp: 92-94 °C; yield: 78.4%; rec.solv.: cyclohexane/benzene ^{1}H NMR ($CDCl_3$) δ 0.72 (d, 3H, $CH(CH_3)_2$, J = 6.7 Hz), 1.08 (d, 3H, $CH(CH_3)_2$, J = 6.5 Hz), 2.45-2.55 (m, 1H, $CH(CH_3)_2$), 3.05 (d, 1H, PhC*H*CO, J = 10.2 Hz), 3.89 (s, 3H, $COCH_3$), 7.30-7.32 (m, 5H, benzene protons), 8.25 (d, 1H, pyridine proton, J = 2.1 Hz), 8.28 (s, 1H, pyridine proton), 8.45 (bs, 1H, CON*H*), 8.82 (d, 1H, pyridine proton, J = 1.4 Hz).

General Procedure for the synthesis of (*E*)-*n*-butyl 3-(6-(arylacetamido)pyridinyl)acrylates 17-19, 20a-f.

Method 1. (**17**): Palladium acetate (0.95 mmol, 0.21 g) was added under nitrogen atmosphere to a solution of N-(6-bromopyridin-2-yl)2-phenylbutanamide **13** (6.8 mmol, 0.22 g), triethylamine (16.73 mmol, 2.32 mL) and *n*-butyl acrylate (20.57 mmol, 2.95 mL) in anhydrous *N,N*-Dimethylacetamide (8 mL) and in a sealed tube. The resulting mixture was stirred at 100°C for 8h. The reaction was quenched by water (30 mL) and extracted with ethyl acetate (3 x 50 mL). The collected organic phases were washed with 2N HCl (3 x 50 mL) and saturated sodium chloride solution (3 x 50 mL), dried and concentrated to obtain an oily residue that was purified by silica gel chromatography eluting with ethyl acetate/n-hexane 1/3 to provide pure **17** as a pale yellow solid.

Method 2. **(18, 20a-f). Example: Synthesis of (*E*)-*n*-butyl 3-(6-(2-(phenyl-1-yl)butanamido)pyridin-3-yl)acrylate (20b).**

Triphenylphosphine (0.22 mmol, 0.06 g) and palladium acetate (0.081 mmol, 0.02 g) were added under nitrogen atmosphere to a solution of *N*-(5-bromopyridin-2-yl)-2-(phenyl-1-yl) butanamide **16b** (4.40 mmol, 1.50 g), sodium bicarbonate (8,79 mmol, 0.74 g), triethylamine (18.90 mmol, 2.6 mL) and *n*-butyl acrylate (5.28 mmol, 0.76 mL) in anhydrous *N,N*-dimethylformamide (5 mL) and in a sealed tube. The resulting mixture was stirred at 100°C for 2h. The reaction was quenched by water (30 mL) and extracted with ethyl acetate (3 x 50 mL). The collected organic phases were washed with 2N HCl (3 x 50 mL) and saturated sodium chloride solution (3 x 50 mL), dried and concentrated to obtain an oily residue that was purified by silica gel chromatography eluting with ethyl acetate/*n*-hexane 1/3 to provide pure **20b** as a pale yellow solid.

Mp: 102-104 °C; yield: 88.2%; rec solv: cyclohexane/benzene ^{1}H-NMR ($CDCl_3$) *δ* 0.91-0.94 (t, 3H, $OCH_2CH_2CH_2CH_3$, J = 7.4 Hz), 0.95-0.98 (t, 3H, CH_2CH_3, J = 7.3 Hz), 1.42-1.44 (m, 2H, $OCH_2CH_2CH_2CH_3$), 1.66-1.70 (m, 2H, $OCH_2CH_2CH_2CH_3$), 1.85-1.87 (m, 2H, CH_2CH_3), 3.42 (t, 1H, PhC*H*CO, J = 6.5 Hz), 4.19-4.22 (t, 2H, $OCH_2CH_2CH_2CH_3$, J = 6.7 Hz), 6.40 (d, 1H, CH_2=CH_2COOBu, J = 16.0 Hz), 7.27-7.36 (m, 5H, benzene protons), 7.59 (d, 1H, CH_2=CH_2COOBu, J = 16.0 Hz), 7.87 (d, 1H, pyridine proton, J = 2.3 Hz), 8.19 (bs, 1H, CON*H*), 8.27 (s, 1H, pyridine proton), 8.30 (d, 1H, pyridine proton, J = 2.5 Hz).

Method 3. (**19**): **butyl (E)-3-(5-(2-phenylbutanamido)pyridin-2-yl)acrylate**

Triphenylphosphine (0.37 mmol, 0.10 g) and palladium acetate (0.18 mmol, 0.04 g) were added under nitrogen atmosphere to a solution of N-(6-bromopyridin-3-yl)-2-phenylbutanamide **15** (4.40 mmol, 1.50 g), sodium acetate trihydrate (11.43 mmol, 1.55 g), water (0.5 mL) and *n*-butyl acrylate (8.79 mmol, 1.26 mL) in anhydrous *N,N*-dimethylformamide (8.5 mL) and in a sealed tube. The resulting mixture was stirred at 140°C overnight. The

reaction was quenched by water (50 mL) and extracted with ethyl acetate (3 x 50 mL). The collected organic phases were washed with saturated sodium chloride solution (100 mL), dried, and concentrated to obtain an oily residue that was purified by silica gel chromatography eluting with ethyl acetate/*n*-hexane 1/3 to provide pure **19** as a pale yellow solid.

General Procedure for the Synthesis of acids 21-23, 24a-f, and 26a-f. Example: 6-(2-phenylbutanamido)nicotinic acid (26c).

A mixture of methyl 6-(2-phenylbutanamido)nicotinate **25c** (0.57 mmol, 0.20g), THF (15 mL), and 2 N KOH (1.14 mmol, 0.48 g) was stirred at room temperature overnight. Afterward, THF was removed under reduced pressure, and the residue was poured into water (50 mL) and extracted with ethyl acetate (3 x 30 mL). The aqueous layer was acidified by adding 2 N HCl at 0 °C; the obtained precipitate was filtered and dried to give compound **26c**.

Mp: 254-256 °C; yield: 95.7%; rec solv: methanol ^{1}H-NMR (DMSO) δ 0.61 (d, 3H, CH(CH_3)$_2$, J = 6.6 Hz), 0.97 (d, 3H, CH(CH_3)$_2$, J = 6.4 Hz), 2.35-2.32 (m, 1H, CH(CH$_3$)$_2$), 3.5 (d, 1H, PhCHCO, J = 10.7 Hz), 7.21 (t, 1H, benzene proton, J = 7.0 Hz), 7.29 (t, 2H, benzene protons, J = 7.3 Hz), 7.37 (d, 2H, benzene protons, J = 7.8 Hz), 8.14-8.17 (m, 2H, pyridine protons), 8.75 (s, 1H, pyridine protons), 11.02 (s, 1H, CONH), 13.21 (s, 1H, COOH).

General procedure for the synthesis of acrylamides 6-8, 9a-f and 11a-f. Example: (*E*)-N-hydroxy-3-(6-(2-(naphthalen-2-yl)acetamido)pyridin-3-yl)acrylamide (9f).

Ethyl chloroformate (1.26 mmol, 0.12 mL) and Et$_3$N (1.37 mmol, 0.19 mL) were added to a cooled (0 °C) solution of (E)-N-hydroxy-3-(6-(2-(naphthalen-2-yl)acetamido)pyridin-3-yl)acrylic acid **24f** (1.05 mmol, 0.42 g) in THF dry (10 mL) and the mixture was stirred for 10 min. The solid was filtered off, and O-(2-methoxy-2-propyl)hydroxylamine (3.15 mmol, 0.23 mL) was added to the filtrate. The solution was stirred for 15 min at 0 °C, then was evaporated under reduced pressure, and the residue was diluted in MeOH (10 mL). Amberlyst 15 ion-exchange resin (0.42 mg) was added to the solution of the O-protected hydroxamate, and the mixture was stirred at RT for 1 h. Afterward, the mixture was filtered, and the filtrate was concentrated in vacuo to give the crude **9f**, which was purified by crystallization.

General procedure for the synthesis of nicotinamides 10a-f and 12a-f. Example: (*E*)-N-(2-aminophenyl)-3-(6-(2-(naphthalen-1-yl)acetamido)pyridin-3-yl)acrylamide (10e).

Et$_3$N (2.24 mmol, 0.31 mL) and BOP reagent (0.67 mmol, 0.30 g) were added under N_2 atmosphere to a solution of (E)-3-(6-(2-(naphthalen-1-yl)acetamido)pyridin-3-yl)acrylic acid **24e** in DMF dry (3 mL), and the resulting mixture was stirred for 30 min at room temperature. After this time, 1,2-phenylendiamine (0.56 mmol, 0.06 g) was added. After the completion of the reaction, the mixture was quenched with water (30 mL) and extracted with ethyl acetate (3 x 30 mL). The combined organic layers were washed with brine, dried over anhydrous sodium sulfate, and concentrated under reduced pressure. The obtained residue was purified by chromatography on silica gel eluting with EtOAc/CHCl$_3$ 1:1 to give compound **10e** as a white solid.

Chemical and physical data of compounds 6-8, 9a-f, 10a-f, 11a-f, 12a-f, 13-15, 16a-f, 17-19, 20a-f, 21-23, 24a-f, 25a-f, 26a-f are in *Supporting info* (Table S1-9).

^{1}H NMR spectral data of compounds 6-8, 9a-f, 10a-f, 11a-f, 12a-f.

(6) (*E*)-*N*-(6-(3-(hydroxyamino)-3-oxoprop-1-en-1-yl)pyridin-2-yl)-2-phenylbutanamide

Mp: 143-145 °C; yield: 67.3%; rec solv: benzene ^{1}H NMR (DMSO) δ 0.82 (t, 3H, PhCHCH$_2$CH_3CO, J = 8 Hz), 1.63-1.67 (m, 1H, PhCHCH_2CH$_3$CO), 2.01-2.05 (m, 1H, PhCHCH_2CH$_3$CO), 3.80 (t, 1H, PhCHCO, J = 8 Hz), 6.76 (d, 1H, PyrCH=CHCO, J = 16 Hz), 7.18-7.37 (m, 7H, PyrCH=CHCO and benzene protons), 7.75 (t, 1H, pyridine proton, J = 8 Hz), 8.01 (d, 1H, pyridine proton, J = 8 Hz), 9.02 (bs, 1H, CONHOH), 10.59 (s, 1H, CONHOH), 10.82 (s, 1H, CONHPyr).

(7) (*E*)-*N*-(5-(3-(hydroxyamino)-3-oxoprop-1-en-1-yl)pyridin-3-yl)-2-phenylbutanamide

Mp: 190-192 °C; yield: 87.0%; rec solv: acetonitrile ^{1}H NMR (DMSO) δ 0.88 (t, 3H, PhCHCH$_2$CH_3CO, J = 7.5 Hz), 1.71-1.78 (m, 1H, PhCHCH_2CH$_3$CO), 2.05-2.12 (m, 1H, PhCHCH_2CH$_3$CO), 3.64 (t, 1H, PhCHCO, J = 7.2 Hz), 6.56 (d, 1H, PyrCH=CHCO, J = 16 Hz), 7.13-7.43 (m, 6H, PyrCH=CHCO and benzene protons), 8.48 (d, 2H, pyridine proton, J = 5 Hz), 8.62 (s, 1H, pyridine proton), 9.03 (bs, 1H, CONHOH), 10.66 (s, 1H, CONHOH), 10.85 (s, 1H, CONHPyr).

(8) (*E*)-*N*-(6-(3-(hydroxyamino)-3-oxoprop-1-en-1-yl)pyridin-3-yl)-2-phenylbutanamide

Mp: 69-71 °C; yield: 59.8%; rec solv: cyclohexane/benzene ^{1}H NMR (DMSO) δ 0.87 (t, 3H, PhCHCH$_2$CH_3CO, J = 7.5 Hz), 1.70-1.77 (m, 1H, PhCHCH_2CH$_3$CO), 2.03-2.08 (m, 1H, PhCHCH_2CH$_3$CO), 3.62 (t, 1H, PhCHCO, J = 8 Hz), 6.80 (d, 1H, PyrCH=CHCO, J = 16 Hz), 7.23-7.42 (m, 6H, PyrCH=CHCO and benzene protons), 7.53 (d, 1H, pyridine proton, J = 8 Hz), 8.08 (d, 1H, pyridine proton, J = 8.3 Hz), 8.77 (s, 1H, pyridine proton), 9.31 (bs, 1H, CONHOH), 10.54 (s, 1H, CONHOH), 10.86 (s, 1H, CONHPyr).

(9a) (*E*)-*N*-hydroxy-3-(6-(2-phenylacetamido)pyridin-3-yl)acrylamide

Mp: 195-197 °C; yield: 67.3%; rec solv: acetonitrile ^{1}H NMR (DMSO) δ 3.70 (s, 2H, PhCH_2CO), 6.42 (d, 1H, PyrCH=CHCO, J = 15.4 Hz), 7.21-7.30 (m, 5H, benzene protons), 7.40 (d, 1H, PyrCH=CHCO, J = 15.5 Hz), 7.94 (d, 1H, pyridine proton, J = 8.4 Hz), 8.06 (d, 1H, pyridine proton, J = 8.5 Hz), 8.46 (s, 1H, pyridine proton), 9.00 (bs, 1H, CONHOH), 10.71 (s, 1H, CONHOH), 10.84 (s, 1H, CONHPyr).

(9b) (*E*)-*N*-hydroxy-3-(6-(2-phenylpropanamido)pyridin-3-yl)acrylamide

Mp: 149-151; yield: 87.0%; rec solv: benzene ^{1}H NMR (DMSO) δ 0.84 (t, 3H, PhCHCH$_2$CH_3CO, J = 7.3 Hz), 1.67-1.71 (m, 1H, PhCHCH_2CH$_3$CO), 2.01-2.04 (m, 1H, PhCHCH_2CH$_3$CO), 3.78 (t, 1H, PhCHCO, J = 8.5 Hz), 6.44 (d, 1H, PyrCH=CHCO, J = 15.9 Hz), 7.21-7.40 (m, 6H, PyrCH=CHCO and benzene protons), 7.95 (d, 1H, pyridine proton, J = 8 Hz), 8.12 (d, 1H, pyridine proton, J = 8.3 Hz), 8.45 (s, 1H, pyridine proton), 9.02 (bs, 1H, CONHOH), 10.73 (s, 1H, CONHOH), 10.82 (s, 1H, CONHPyr).

(9c) (*E*)-*N*-(5-(3-(hydroxyamino)-3-oxoprop-1-en-1-yl)pyridin-2-yl)-3-methyl-2 phenylbutanamide

Mp: 178-180; yield: 59.8%; rec solv: acetonitrile ^{1}H NMR (DMSO) δ 0.61 (bs, 3H, CH_3CHCH$_3$), 0.96 (t, 3H, CH$_3$CHCH_3), 2.32 (m, 1H, CH$_3$CHCH$_3$), 3.05 (m, 1H, PhCHCO), 6.41 (d, 1H, PyrCH=CHCO, J = 0.6 Hz), 7.19-7.37 (m, 6H, PyrCH=CHCO and benzene protons), 7.93 (d, 1H, pyridine proton, J = 1.5 Hz), 8.08 (s, 1H, pyridine proton), 8.41 (s, 1H, pyridine proton), 9.01 (bs, 1H, CONHOH), 10.70 (s, 1H, CONHOH), 10.83 (s, 1H, CONHPyr).

(9d) (*E*)-3-(6-(2,3-diphenylpropanamido)pyridin-3-yl)-*N*-hydroxyacrylamide

Mp: 201-203 °C; yield: 78.5%; rec solv: acetonitrile/methanol ^{1}H NMR (DMSO) δ 2.90-2.95 (m, 1H, CHCH_2Ph), 3.36-3.42 (m, 1H, CHCH_2Ph), 4.25-4.27 (m, 1H, PhCHCO), 6.40 (d, 1H, PyrCH=CHCO, J = 16.0 Hz), 7.10-7.43 (m, 11H, benzene protons and PyrCH=CHCO), 7.92 (d, 1H, pyridine proton, J = 8.0 Hz), 8.04 (d, 1H, pyridine proton, J = 8.0 Hz), 8.40 (s, 1H, pyridine proton), 9.00 (bs, 1H, CONHOH), 10.67 (s, 1H, CONHOH), 10.78 (s, 1H, CONHPyr).

(9e) (*E*)-*N*-hydroxy-3-(6-(2-(naphthalen-1-yl)acetamido)pyridin-3-yl)acrylamide

Mp: 212-214°C; yield: 68.4%; rec solv: acetonitrile/methanol ^{1}H NMR (DMSO) δ 4.22 (s, 2H, NaphtCH_2CO), 6.42 (d, 1H, PyrCH=CHCO, J = 8.0 Hz), 7.40-7.52 (m, 6H, PyrCH=CHCO and aromatic protons), 7.82 (d, 1H, aromatic proton, J = 4.0 Hz), 7.89-7.94 (m, 1H, aromatic protons), 8.03 (d, 1H, pyridine proton, J = 4 Hz), 8.09 (d, 1H, pyridine proton, J = 8.0 Hz), 8.49 (s, 1H, pyridine proton), 9.01 (bs, 1H, CONHOH), 10.71 (s, 1H, CONHOH), 10.99 (s, 1H, CONHPyr).

(9f) (*E*)-*N*-hydroxy-3-(6-(2-(naphthalen-2-yl)acetamido)pyridin-3-yl)acrylamide

Mp: 167-169°C; yield: 65.7%; rec solv: benzene/acetonitrile ^{1}H NMR (DMSO) δ 3.89 (s, 2H, NaphtCH_2CO), 6.44 (d, 1H, PyrCH=CHCO, J = 16.0 Hz), 7.38-7.50 (m, 4H, PyrCH=CHCO and aromatic protons), 7.85-7.94 (m, 4H, aromatic proton), 7.95 (d, 1H, pyridine proton, J = 4.0 Hz), 8.07 (d, 1H,

pyridine proton, J = 4.0 Hz), 8.47 (s, 1H, pyridine proton), 10.03 (bs, 1H,CONHO*H*), 10.85 (s, 1H, CON*H*OH), 10.97 (s, 1H, CON*H*Pyr).

(10a) (*E*)-*N*-(2-aminophenyl)-3-(6-(2-phenylacetamido)pyridin-3-yl)acrylamide

Mp: 215-217°C; yield: 61.3%; rec solv: acetonitrile/methanol ^{1}H NMR (DMSO) δ 3.71-3.74 (m, 2H, PhCH_2CO), 4.97 (bs, 2H, PhNH_2), 6.54 (d, 1H, PyrCH=C*H*CO, J = 8.0 Hz), 6.72 (d, 1H, PyrC*H*=CHCO, J = 8.0 Hz), 6.90 (m, 1H, aniline proton), 7.21-7.24 (m, 5H, benzene protons), 7.31-7.32 (m, 1H, aromaric proton), 7.34-7-35 (m, 1H, aromatic proton), 7.52-7.53 (m, 3H, aromatic proton), 8.79 (s, 1H, pyridine proton), 9.34 (s, 1H, CON*H*Pyr), 10.90 (s, 1H, CON*H*aniline).

(10b) (*E*)- *N*-(2-aminophenyl)-3-(6-(2-phenylpropanamido)pyridin-3-yl)acrylamide

Mp: 172-174°C; yield: 77.4%; rec solv: acetonitrile ^{1}H NMR (DMSO) δ 0.85 (t, 3H, PhCHCH$_2$CH_3CO, 7.2 Hz), 1.69-1.72 (m, 1H, PhCHCH_2CH$_3$CO), 2.05-2.09 (m, 1H, PhCHCH_2CH$_3$CO), 3.81 (t, 1H, PhC*H*CO, J = 4.0 Hz), 4.93 (bs, 2H, PhNH_2), 6.57 (t, 1H, aniline proton, J = 16.0 Hz), 6.74 (d, 1H, aniline proton, J = 8.0 Hz), 6.87-6.93 (m, 2H, PyrCH=C*H*CO and aniline proton), 7.22-7.25 (m, 1H, aniline proton), 7.30-7.54 (m, 5H, benzene protons + 1H PyrC*H*=CHCO), 8.01 (d, 1H, pyridine proton, J = 8.0 Hz), 8.17 (d, 1H, pyridine róton, J = 12.0 Hz), 8.52 (s, 1H, pyridine proton), 9.36 (s, 1H, CON*H*Pyr), 10.87 (s, 1H, CON*H* aniline).

(10c) (*E*)-*N*-(5-(3-((2-aminophenyl)amino)-3-oxoprop-1-en-1-yl)pyridin-2-yl)-3-methyl-2-phenylbutanamide

Mp: 204-206°C; yield: 59.2%; rec solv: acetonitrile/methanol ^{1}H NMR (DMSO) δ 0.62 (d, 3H, CH_3CHCH$_3$, J = 8.0 Hz), 0.98 (d, 3H, CH$_3$CHCH_3, J = 4.0 Hz), 2.30-2.33 (m, 1H, CH$_3$C*H*CH$_3$), 3.48 (d, 1H, PhC*H*CO, J = 12 Hz), 4.91 (bs, 2H, PhNH_2), 6.54 (t, 1H, aniline proton, J = 12.0 Hz), 6.71 (d, 1H, aniline proton, J = 8.0 Hz), 6.83-6.89 (m, 2H, PyrCH=C*H*CO and aniline proton), 7.20-7.22 (m, 1H, aniline proton), 7.27-7.39 (m, 5H, benzene protons), 7.49 (d, 1H, PyrC*H*=CHCO, J = 16.0 Hz), 7.97 (d, 1H, pyridine proton, J = 8.0 Hz), 8.14 (d, 1H, pyridine proton, J = 12.0 Hz), 8.49 (s, 1H, pyridine proton), 9.32 (s, 1H, CON*H*Pyr), 10.86 (bs, 1H, CON*H*aniline).

(10d) (*E*)-*N*-(2-aminophenyl)-3-(6-(2,3-diphenylpropanamido)pyridin-3-yl)acrylamide

Mp: 180-182°C; yield: 78.5%; rec solv: acetonitrile ^{1}H NMR (DMSO) δ 2.90-2.95 (m, 1H, CHCH_2Ph), 3.37-3.41 (m, 1H, CHCH_2Ph), 4.27-4.29 (m, 1H, PhC*H*CO), 4.90 (bs, 2H, PhNH_2), 6.53 (t, 1H, aniline proton, J = 8.0 Hz), 6.71 (d, 1H, aniline proton, J = 8.0 Hz), 6.82-6.87 (m, 2H, PyrCH=C*H*CO and aniline proton), 7.11-7.12 (m, 1H, aniline proton), 7.19-7.22 (m, 5H, benzene protons), 7.27-7.31 (m, 3H, benzene protons), 7.42-7.48 (m, 3H, PyrC*H*=CHCO and benzene protons), 7.96 (d, 1H, pyridine proton, J = 8.0 Hz), 8.09 (d, 1H, pyridine proton, J = 8.0 Hz), 8.45 (s, 1H, pyridine proton), 9.32 (s, 1H, CON*H*Pyr), 10.82 (s, 1H, CON*H*aniline).

(10e) (*E*)-*N*-(2-aminophenyl)-3-(6-(2-(naphthalen-1-yl)acetamido)pyridin-3-yl)acrylamide

Mp: 155-157°C; yield: 58.3%; rec solv: benzene/acetonitrile ^{1}H NMR (DMSO) δ 4.23 (s, 2H, NaphtCH_2CO), 4.90 (bs, 2H, PhNH_2), 6.53 (t, 1H, aniline proton, J = 8.0 Hz), 6.71 (d, 1H, aniline proton, J = 8.0 Hz), 6.84-6.87 (m, 2H, aniline protons), 7.30 (d, 1H, PyrCH=C*H*CO, J = 8.0 Hz), 7.43-7.55 (m, 5H, aromatic protons), 7.82 (d, 1H, PyrC*H*=CHCO, J = 8.0 Hz), 7.91 (d, 1H, aromatic proton, J = 8.0 Hz), 7.98 (d, 1H, aromatic proton, J = 4.0 Hz), 8.06-8.12 (m, 2H, pyridine protons), 8.54 (s, 1H, pyridine proton), 9.33 (s, 1H, CON*H*Pyr), 11.02 (s, 1H, CON*H*aniline).

(10f) (*E*)-*N*-(2-aminophenyl)-3-(6-(2-(naphthalen-2-yl)acetamido)pyridin-3-yl)acrylamide

Mp: 238-240°C; yield: 72.8%; rec solv: acetonitrile/methanol ^{1}H NMR (DMSO) δ 3.90 (s, 2H, NaphtCH_2CO), 4.91 (bs, 2H, PhNH_2), 6.54 (t, 1H, aniline proton, J = 4.0 Hz), 6.71 (d, 1H, aniline proton, J = 8.0 Hz), 6.84-6.88 (m, 2H, PyrCH=C*H*CO and aniline proton), 7.30-7.31 (m, 1H, aniline proton), 7.48-7.53 (m, 4H, PyrC*H*=CHCO and aromatic protons), 7.82-7.86 (m, 4H, aromatic protons), 8.00 (d, 1H, pyridine proton, J = 4.0 Hz), 8.10 (d, 1H, pyridine proton, J = 4.0 Hz), 8.53 (s, 1H, pyridine proton), 9.34 (s, 1H, CON*H*Pyr), 10.97 (s, 1H, CON*H*aniline).

(11a) *N*-hydroxy-6-(2-phenylacetamido)nicotinamide

Mp: 199-201°C; yield: 67.3%; rec solv: acetonitrile ^{1}H NMR (DMSO) δ 3.71 (s, 2H, PhCH_2CO), 7.21-7.30 (m, 5H, benzene protons), 8.06 (s, 2H, pyridine proton), 8.64 (s, 1H, pyridine proton), 9.07 (bs, 1H, NHO*H*), 10.94 (s, 1H, N*H*OH), 11.22 (s, 1H, CON*H*Pyr).

(11b) *N*-hydroxy-6-(2-phenylpropanamido)nicotinamide

Mp: 169-171°C; yield: 87.0%; rec solv: benzene/acetonitrile ^{1}H NMR (DMSO) δ 0.81 (t, 3H, PhCHCH$_2$CH_3, J = 16.0 Hz), 1.65-1.68 (m, 1H, PhCHCH_2CH$_3$CO), 2.01-2.04 (m, 1H, PhCHCH_2CH$_3$CO), 3.76 (t, 1H, PhC*H*CO, J = 16.0 Hz), 7.20-7.37 (m, 5H, benzene protons), 8.05 (d, 1H, pyridine proton, J = 12.0 Hz), 8.10 (d, 1H, pyridine proton, J = 12.0 Hz), 8.62 (s, 1H, pyridine proton), 9.05 (bs, 1H, NHO*H*), 10.90 (s, 1H, N*H*OH), 11.21 (s, 1H, CON*H*Pyr).

(11c) *N*-hydroxy-6-(3-methyl-2-phenylbutanamido)nicotinamide

Mp: 132-134°C; yield: 59.8%; rec solv: benzene ^{1}H NMR (DMSO) δ 0.62 (d, 3H, CH_3CHCH$_3$, J = 4.0 Hz), 0.97 (d, 3H, CH$_3$CHCH_3, J = 4.0 Hz), 2.35-2.37 (m, 1H, CH$_3$C*H*CH$_3$), 3.47 (d, 1H, PhC*H*CO, J = 8.0 Hz), 7.20-7.38 (m, 5H, benzene protons), 8.04 (d, 1H, pyridine proton, J = 8.0 Hz), 8.09 (d, 1H, pyridine proton, J = 8.0 Hz), 8.62 (s, 1H, pyridine proton), 9.10 (bs, 1H, NHO*H*), 10.91 (s, 1H, N*H*OH), 11.15 (s, 1H,CON*H*Pyr).

(11d) 6-(2,3-diphenylpropanamido)-*N*-hydroxynicotinamide

Mp: 195-197°C; yield: 78.5%; rec solv: acetonitrile ^{1}H NMR (DMSO) δ 2.91-2.95 (m, 1H, CHCH_2Ph), 3.37-3.41 (m, 1H, CHCH_2Ph), 4.24-4.26 (m, 1H, PhC*H*CO), 7.10-7.43 (m, 10H, benzene protons), 8.04 (d, 1H, pyridine proton, J = 4.0 Hz), 8.09 (d, 1H, pyridine proton, J = 8.0 Hz), 8.58 (s, 1H, pyridine proton), 9.10 (bs, 1H,NHO*H*), 10.87 (s, 1H, N*H*OH), 11.20 (s, 1H,CON*H*Pyr).

(11e) *N*-hydroxy-6-(2-(naphthalen-1-yl)acetamido)nicotinamide

Mp: 221-223°C; yield: 68.4%; rec solv: acetonitrile/methanol ^{1}H NMR (DMSO) δ 4.24 (s, 2H, NaphtCH_2CO), 7.49-8.09 (m, 7H, aromatic protons), 8.17 (d, 1H, pyridine proton, J = 4.0 Hz), 8.67 (d, 1H, pyridine proton, J = 4.0 Hz), 8.82 (s, 1H, pyridine proton), 9.08 (bs, 1H, NHO*H*), 11.08 (s, 1H,N*H*OH), 11.22 (s, 1H,CON*H*Pyr).

(11f) *N*-hydroxy-6-(2-(naphthalen-2-yl)acetamido)nicotinamide

Mp: 217-219°C; yield: 65.7%; rec solv: acetonitrile/methanol ^{1}H NMR (DMSO) δ 3.92 (s, 2H, NaphtCH_2CO), 7.46-8.01 (m, 7H, aromatic protons), 8.07 (d, 1H, pyridine proton, J = 4.0 Hz), 8.11 (d, 1H, pyridine proton, J = 4.0 Hz), 8.65 (s, 1H, pyridine proton), 9.08 (bs, 1H, NHO*H*), 11.02 (s, 1H, N*H*OH), 11.22 (s, 1H, CON*H*Pyr).

(12a) *N*-(2-aminophenyl)-6-(2-phenylacetamido)nicotinamide

Mp: 238-240°C; yield: 61.3%; rec solv: acetonitrile/methanol ^{1}H NMR (DMSO) δ 3.73 (s, 2H, PhCH_2CO), 4.91 (bs, 2H, PhNH_2), 6.55 (t, 1H, aniline proton, J = 4.0 Hz), 6.73 (d, 1H, aniline proton, J = 8.0 Hz), 6.94 (t, 1H, aniline proton, J = 8.0 Hz), 7.22 (d, 1H, aniline proton, J = 8.0 Hz), 7.28-7.32 (m, 5H, benzene protons), 8.12 (d, 1H, pyridine proton, J = 8.0 Hz), 8.28 (d, 1H, pyridine proton, J = 8.0 Hz), 8.89 (s, 1H, pyridine proton), 9.67 (s, 1H, CON*H*Pyr), 11.00 (s, 1H, CON*H*aniline).

(12b) *N*-(2-aminophenyl)-6-(2-phenylpropanamido)nicotinamide

Mp: 98-100°C; yield: 77.4%; rec solv: cyclohexane/benzene ^{1}H NMR (DMSO) δ 0.82 (t, 3H, PhCHCH$_2$CH_3CO, J = 16.0 Hz), 1.68-1.70 (m, 1H, PhCHCH_2CH$_3$CO), 2.05-2.07 (m, 1H, PhCHCH_2CH$_3$CO), 3.79 (t, 1H, PhC*H*CO, J = 16.0 Hz), 4.90 (bs, 2H, PhNH_2), 6.56 (t, 1H, aniline proton, J = 8.0 Hz), 6.73 (d, 1H, aniline proton, J = 8.0 Hz), 6.93 (t, 1H, aniline proton, J = 4.0 Hz), 7.11 (d, 1H, aniline proton, J = 8.0 Hz), 7.21-7.39 (m, 5H, benzene protons), 8.15 (d, 1H, pyridine proton, J = 8.0 Hz), 8.29 (d, 1H, pyridine proton, J = 12.0 Hz), 8.87 (s, 1H, pyridine proton), 9.67 (s, 1H, CON*H*Pyr), 10.96 (s, 1H, CON*H*aniline).

(12c) *N*-(2-aminophenyl)-6-(3-methyl-2-phenylbutanamido)nicotinamide

Mp: 110-112°C; yield: 59.2%; rec solv: cyclohexane/benzene ^{1}H NMR (DMSO) δ 0.71 (d, 3H, C*H*$_3$CHCH$_3$, J = 8.0 Hz), 1.07 (d, 3H, CH$_3$CHC*H*$_3$, J = 8.0 Hz), 2.45-2.47 (m, 1H, CH$_3$C*H*CH$_3$), 3.03 (d, 1H, PhC*H*CO, J = 4.0 Hz), 4.90 (bs, 2H, PhN*H*$_2$), 6.78-6.80 (m, 2H, aniline protons), 7.03-7.06 (m, 1H, aniline proton), 7.24-7.33 (m, 6H, benzene protons and aniline proton), 8.01 (d, 1H, pyridine proton, J = 4.0 Hz), 8.22 (d, 1H, pyridine proton, J = 4.0 Hz), 8.37 (s, 1H, pyridine proton), 8.70 (s, 1H, CON*H*Pyr), 9.92 (bs, 1H, CON*H* aniline).

(12d) *N*-(2-aminophenyl)-6-(2,3-diphenylpropanamido)nicotinamide
Mp: 186-188°C; yield: 78.5%; rec solv: acetonitrile ^{1}H NMR (DMSO) δ 2.93-2.98 (m, 1H, CHC*H*$_2$Ph), 3.38-3.43 (m, 1H, CHC*H*$_2$Ph), 4.26-4.30 (m, 1H, PhC*H*CO), 4.89 (bs, 2H, PhN*H*$_2$), 6.54 (t, 1H, aniline proton, J = 8.0 Hz), 6.73 (d, 1H, aniline proton, J = 8.0 Hz), 6.92 (t, 1H, aniline proton, J = 8.0 Hz), 7.11 (d, 2H, aniline proton and benzene proton, J = 12.0 Hz), 7.19-7.23 (m, 5H, benzene protons), 7.28-7.32 (m, 2H, benzene protons), 7.43-7.45 (m, 2H, benzene protons), 8.11 (d, 1H, pyridine proton, J = 8.0 Hz), 8.26 (d, 1H, pyridine proton, J = 8.0 Hz), 8.83 (s, 1H, pyridine proton), 9.64 (s, 1H, CON*H*Pyr), 10.93 (s, 1H, CON*H*aniline).

(12e) *N*-(2-aminophenyl)-6-(2-(naphthalen-1-yl)acetamido)nicotinamide
Mp: 218-220°C; yield: 58.3%; rec solv: acetonitrile/methanol ^{1}H NMR (DMSO) δ 4.25 (s, 2H, NaphtC*H*$_2$CO), 4.91 (bs, 2H, PhN*H*$_2$), 6.55 (t, 1H, aniline proton, J = 16.0 Hz), 6.74 (d, 1H, aniline proton, J = 12.0 Hz), 6.94 (t, 1H, aniline proton, J = 16.0 Hz), 7.11 (d, 1H, aniline proton, J = 8.0 Hz), 7.44-7.53 (m, 4H, aromatic protons), 7.83 (d, 1H, aromatic protons, J = 8.0 Hz), 7.91 (d, 1H, aromatic protons, J = 8.0 Hz), 8.07-8.12 (m, 2H, aromatic proton and pyridine proton), 8.27 (d, 1H, pyridine proton, J = 8.0 Hz), 8.53 (s, 1H, pyridine proton), 8.91 (s, 1H, CON*H*Pyr), 11.16 (s, 1H, CON*H*aniline).

(12f) *N*-(2-aminophenyl)-6-(2-(naphthalen-2-yl)acetamido)nicotinamide
Mp: >250°C; yield: 72.8%; rec solv: methanol ^{1}H NMR (DMSO) δ 3.92 (s, 2H, NaphtC*H*$_2$CO), 4.90 (bs, 2H, PhN*H*$_2$), 6.55 (t, 1H, aniline proton, J = 16.0 Hz), 6.74 (d, 1H, aniline proton, J = 12.0 Hz), 6.94 (t, 1H, aniline proton, J = 12.0 Hz), 7.11 (d, 1H, aniline proton, J = 8.0 Hz), 7.46-7.50 (m, 3H, aromatic protons), 7.83-7.86 (m, 4H, aromatic protons), 8.13 (d, 1H, pyridine proton, J = 8.0 Hz), 8.28 (d, 1H, pyridine proton, J= 8.0 Hz), 8.90 (s, 1H, pyridine proton), 9.66 (s, 1H, CON*H*Pyr), 11.08 (s, 1H, CON*H*aniline).

Mouse HDAC1 Enzyme Assay: For inhibition assay, partially purified HDAC1 from mouse A20 cells (ATCC: TIB208) (anion exchange chromatography, affinity chromatography) was used as enzyme source. HDAC activity was determined as described [19] using [^{3}H] acetate-prelabeled chicken reticulocyte histones as substrate. 50 µL of mouse HDAC1 enzyme fractions were incubated with different concentrations of compounds for 15 min on ice, and 10 µL of total [^{3}H] acetate-prelabeled chicken reticulocyte histones (4 mg/mL) were added, resulting in a concentration of 41 µM. The mixture was incubated at 37 °C for 1 h. The reaction was stopped by the addition of 50 µL of 1 M HCl/0.4 M acetylacetate and 1 mL ethyl acetate. After centrifugation at 10000g for 5 min, an aliquot of 600 µL of the upper phase was counted for radioactivity in 3 mL of liquid scintillation cocktail.

HDAC1, -3, -4, -6, -8 isoform inhibition assay: The described compounds were tested against purified hrHDAC1, -3, -4, -6, and -8 in 10-dose IC_{50} mode with 3-fold serial dilution starting from 100 µM solutions. Three fluorogenic peptides, from p53 residues 379-382 (RHKK(Ac)AMC) (for HDAC1, -3, -6), or the fluorogenic class IIa (Boc-Lys(trifluoroacetyl)-AMC) substrate (for HDAC4) [20] the diacetylated p53 residues 379-382 (RHK(Ac)K(Ac)AMC) (for HDAC8) were used as substrates, and SAHA was employed as reference compound and positive control. Deacetylated peptides were sensitive towards lysine peptidase, and free fluorogenic 4-methylcoumarin-7-amide (MCA) was generated, which can be excited at 355 nm and observed at 460 nm. The data were analyzed on a plate to plate basis in relationship to the control and imported into analytical software. IC_{50} values were calculated using the GraphPad Prism 4 program based on a sigmoidal dose-response equation.

Cellular assays

Cell lines and cultures: U937 were grown as described in [16h] whereas K562, A549, and HCT116 cells were maintained as reported in **[16j]**

Cell-cycle analysis using U937 cells: 2.5x10^5 cells were harvested and resuspended in 500 mL hypotonic buffer (0.1 % Triton X-100, 0.1 % sodium citrate, 50 mg mL^{-1} propidium iodide (PI), RNAse A). Cells were incubated in the dark for 30 min.. Cell death was measured as percentage of cells in pre-G1 phase of the cell cycle. Samples were measured on a FACS-Calibur flow cytometer using the Cell Quest software (Becton Dickinson) and processed with the Cell Quest software (Becton Dickinson) and ModFit LT ver. 3 software (Verity) as previously reported [16h, 21]. All experiments were performed three times.

Granulocytic differentiation in U937 cells: Granulocytic differentiation was carried out as previously described [16h, 22]. Briefly, U937 cells were harvested and resuspended in 10mL phycoerythrin-conjugated CD11c (CD11c-PE). Control samples were incubated with 10 mL PE-conjugated mouse IgG1 for 30 min at 4°C in the dark, washed in PBS, and resuspended in 500 mL PBS containing PI (0.25 µg mL^{-1}). Samples were analyzed by FACS with Cell Quest technology (Becton Dickinson). PI-positive cells were excluded from the analysis.

Antiproliferative activity: The antiproliferative effect of the HDAC inhibitors on cell proliferation was evaluated against K562 (chronic myeloid carcinoma), A549 (non-small-cell lung cancer), and HCT-116 (human colon cancer) tumor cell lines using the CellTiter-Glo luminescent cell viability assay (Promega, Madison, WI) according to the manufacturer's instructions. K562, A549, and HCT-116 cells, in exponential growth, were incubated for 72 h at different concentrations of the inhibitors. Then an equivalent of the CellTiter-Glo reagent was added, the solution was mixed for 2 min in order to induce cell lysis, and the luminescence was recorded after a further 10 min. The IC_{50} was calculated using GraphPad software **[16j]**.

Histone Extraction: After stimulation with compounds, U937 cells were collected by centrifugation and washed two times with PBS. Then the samples were resuspended in Triton extraction buffer [TEB; PBS containing 0.5% Triton X-100 (v/v), 2 mM PMSF, and 0.02% (w/v) NaN3)], and the lysis was performed for 10 min at 4 °C. Next, samples were centrifugated at 2000 rpm for 10 min at 4 °C, and the pellets were washed in TEB (half the volume). After a new centrifugation under the same conditions, the samples were resuspended in 0.2 N HCl and the acidic histone extraction was carried out overnight at 4 °C.

Total proteins extraction: U937 cells were harvested and washed once with cold PBS and lysed in a lysis buffer containing 50mM Tris-HCl pH 7.4, 150mM NaCl, 1%NP40, 10mM NaF, 1mM PMSF (phenyl-methylsulphonylfluoride) and protease inhibitor cocktail (Roche). The lysates were centrifuged at 13000 rpm for 30 min at 4°C. Protein concentrations were estimated by Bradford assay (Bio-Rad).

Western Blot Analysis: 30 µg total protein and 2 µg histone extracts were denatured and boiled in buffer (0.25 M Tris-HCl, pH 6.8, 8% SDS, 40% glycerol, 5% 2-mercaptoethanol, and 0.05% bromophenol blue) for 3 min before electrophoresis. Proteins were subjected to sodium dodecyl sulfate-polyacrylamide gel electrophoresis in Tris-glycine–SDS buffer (25 mM Tris, 192 mM glycine 0.1% SDS). After electrophoresis, total proteins and histones were transferred to nitrocellulose membranes (Bio-Rad mini-protean gel and Transblot Turbo transfer system, Bio-Rad).
The employed antibodies were acetylated histone H3 (Millipore, 06-599) and Acetyl-tubulin (SIGMA, T7451). Total H4 (Cell Signaling, 2935S) was used to normalize for equal loading of histone extracts, while GAPDH (Santa Cruz, sc-47724) was used to normalize for equal loading of total protein extraction

Acknowledgments

This work was supported by Ricerca Finalizzata 2013 PE-2013-02355271, AIRC 2016 (n. 19162), Vanvitelli per la Ricerca "AdipCare" (ID 263), Campania Regional Government Technology Platform Lotta alle Patologie Oncologiche: iCURE (B21C17000030007), Campania Regional Government FASE2: IDEAL (B63D18000560007), MIUR, Proof of Concept POC01_00043, VALERE 2020 "NETWINS" funds.

Keywords: chromatin • histone deacetylase inhibitors • cancer• apoptosis • cell differentiation

[1] M. Berdasco, M. Esteller, *Hum Genet* **2013**, *132*, 359-383.
[2] T. C. S. Ho, A. H. Y. Chan, A. Ganesan, *J Med Chem* **2020**.
[3] J. E. Bolden, M. J. Peart, R. W. Johnstone, *Nat Rev Drug Discov* **2006**, *5*, 769-784.
[4] aS. Zimmermann, F. Kiefer, M. Prudenziati, C. Spiller, J. Hansen, T. Floss, W. Wurst, S. Minucci, M. Gottlicher, *Cancer Res* **2007**, *67*, 9047-9054; bK. J. Falkenberg, R. W. Johnstone, *Nat Rev Drug Discov* **2014**, *13*, 673-691; cC. Zwergel, S. Valente, C. Jacob, A. Mai, *Expert Opin Drug Discov* **2015**, *10*, 599-613; dS. Minucci, P. G. Pelicci, *Nat Rev Cancer* **2006**, *6*, 38-51; eG. S. Hailu, D. Robaa, M. Forgione, W. Sippl, D. Rotili, A. Mai, *J Med Chem* **2017**, *60*, 4780-4804; fR. Fioravanti, N. Mautone, A. Rovere, D. Rotili, A. Mai, *Curr Opin Chem Biol* **2020**, *57*, 65-74.
[5] W. S. Xu, R. B. Parmigiani, P. A. Marks, *Oncogene* **2007**, *26*, 5541-5552.
[6] aA. Zecchin, L. Pattarini, M. I. Gutierrez, M. Mano, A. Mai, S. Valente, M. P. Myers, S. Pantano, M. Giacca, *J Mol Cell Biol* **2014**, *6*, 116-127; bH. M. Hesham, D. S. Lasheen, K. A. M. Abouzid, *Med Res Rev* **2018**, *38*, 2058-2109; cG. Stazi, R. Fioravanti, A. Mai, A. Mattevi, S. Valente, *Curr Opin Chem Biol* **2019**, *50*, 89-100.
[7] M. Mottamal, S. Zheng, T. L. Huang, G. Wang, *Molecules* **2015**, *20*, 3898-3941.
[8] aT. Eckschlager, J. Plch, M. Stiborova, J. Hrabeta, *Int J Mol Sci* **2017**, *18*; bJ. H. Lee, M. L. Choy, P. A. Marks, *Adv Cancer Res* **2012**, *116*, 39-86.
[9] M. Duvic, J. Vu, *Expert Opin Investig Drugs* **2007**, *16*, 1111-1120.
[10] C. Grant, F. Rahman, R. Piekarz, C. Peer, R. Frye, R. W. Robey, E. R. Gardner, W. D. Figg, S. E. Bates, *Expert Rev Anticancer Ther* **2010**, *10*, 997-1008.
[11] R. M. Poole, *Drugs* **2014**, *74*, 1543-1554.
[12] K. P. Garnock-Jones, *Drugs* **2015**, *75*, 695-704.
[13] S. Valente, A. Mai, *Expert Opin Ther Pat* **2014**, *24*, 401-415.
[14] C. De Souza, B. P. Chatterji, *Recent Pat Anticancer Drug Discov* **2015**, *10*, 145-162.
[15] aC. L. Hamblett, J. L. Methot, D. M. Mampreian, D. L. Sloman, M. G. Stanton, A. M. Kral, J. C. Fleming, J. C. Cruz, M. Chenard, N. Ozerova, A. M. Hitz, H. Wang, S. V. Deshmukh, N. Nazef, A. Harsch, B. Hughes, W. K. Dahlberg, A. A. Szewczak, R. E. Middleton, R. T. Mosley, J. P. Secrist, T. A. Miller, *Bioorg Med Chem Lett* **2007**, *17*, 5300-5309; bJ. L. Methot, P. K. Chakravarty, M. Chenard, J. Close, J. C. Cruz, W. K. Dahlberg, J. Fleming, C. L. Hamblett, J. E. Hamill, P. Harrington, A. Harsch, R. Heidebrecht, B. Hughes, J. Jung, C. M. Kenific, A. M. Kral, P. T. Meinke, R. E. Middleton, N. Ozerova, D. L. Sloman, M. G. Stanton, A. A. Szewczak, S. Tyagarajan, D. J. Witter, J. P. Secrist, T. A. Miller, *Bioorg Med Chem Lett* **2008**, *18*, 973-978; cJ. L. Methot, D. M. Hoffman, D. J. Witter, M. G. Stanton, P. Harrington, C. Hamblett, P. Siliphaivanh, K. Wilson, J. Hubbs, R. Heidebrecht, A. M. Kral, N. Ozerova, J. C. Fleming, H. Wang, A. A. Szewczak, R. E. Middleton, B. Hughes, J. C. Cruz, B. B. Haines, M. Chenard, C. M. Kenific, A. Harsch, J. P. Secrist, T. A. Miller, *ACS Med Chem Lett* **2014**, *5*, 340-345.
[16] aA. Mai, S. Massa, R. Ragno, I. Cerbara, F. Jesacher, P. Loidl, G. Brosch, *J Med Chem* **2003**, *46*, 512-524; bA. Mai, S. Massa, R. Pezzi, S. Simeoni, D. Rotili, A. Nebbioso, A. Scognamiglio, L. Altucci, P. Loidl, G. Brosch, *J Med Chem* **2005**, *48*, 3344-3353; cA. Mai, S. Massa, R. Pezzi, S. Valente, P. Loidl, G. Brosch, *Med Chem* **2005**, *1*, 245-254; dA. Mai, S. Massa, D. Rotili, S. Simeoni, R. Ragno, G. Botta, A. Nebbioso, M. Miceli, L. Altucci, G. Brosch, *J Med Chem* **2006**, *49*, 6046-6056; eA. Mai, S. Valente, A. Nebbioso, S. Simeoni, R. Ragno, S. Massa, G. Brosch, F. De Bellis, F. Manzo, L. Altucci, *Int J Biochem Cell Biol* **2009**, *41*, 235-247; fA. Nebbioso, F. Manzo, M. Miceli, M. Conte, L. Manente, A. Baldi, A. De Luca, D. Rotili, S. Valente, A. Mai, A. Usiello, H. Gronemeyer, L. Altucci, *EMBO Rep* **2009**, *10*, 776-782; gS. Valente, M. Conte, M. Tardugno, S. Massa, A. Nebbioso, L. Altucci, A. Mai, *ChemMedChem* **2009**, *4*, 1411-1415; hS. Valente, M. Tardugno, M. Conte, R. Cirilli, A. Perrone, R. Ragno, S. Simeoni, A. Tramontano, S. Massa, A. Nebbioso, M. Miceli, G. Franci, G. Brosch, L. Altucci, A. Mai, *ChemMedChem* **2011**, *6*, 698-712; iF. Thaler, A. Colombo, A. Mai, R. Amici, C. Bigogno, R. Boggio, A. Cappa, S. Carrara, T. Cataudella, F. Fusar, E. Gianti, S. J. di Ventimiglia, M. Moroni, D. Munari, G. Pain, N. Regalia, L. Sartori, S. Vultaggio, G. Dondio, S. Gagliardi, S. Minucci, C. Mercurio, M. Varasi, *J Med Chem* **2010**, *53*, 822-839; jF. Thaler, M. Varasi, A. Colombo, R. Boggio, D. Munari, N. Regalia, M. G. Rozio, V. Reali, A. E. Resconi, A. Mai, S. Gagliardi, G. Dondio, S. Minucci, C. Mercurio, *ChemMedChem* **2010**, *5*, 1359-1372; kF. Thaler, M. Varasi, A. Abate, G. Carenzi, A. Colombo, C. Bigogno, R. Boggio, R. D. Zuffo, D. Rapetti, A. Resconi, N. Regalia, S. Vultaggio, G. Dondio, S. Gagliardi, S. Minucci, C. Mercurio, *Eur J Med Chem* **2013**, *64*, 273-284; lS. Panella, M. E. Marcocci, I. Celestino, S. Valente, C. Zwergel, D. D. Li Puma, L. Nencioni, A. Mai, A. T. Palamara, G. Simonetti, *Future Med Chem* **2016**, *8*, 2017-2031.
[17] S. Massa, A. Mai, G. Sbardella, M. Esposito, R. Ragno, P. Loidl, G. Brosch, *J Med Chem* **2001**, *44*, 2069-2072.
[18] aJ. I. Rotter, J. M. Diamond, *Nature* **1987**, *329*, 289-290; bD. Buonvicino, R. Felici, G. Ranieri, R. Caramelli, A. Lapucci, L. Cavone, M. Muzzi, L. Di Pietro, C. Bernardini, C. Zwergel, S. Valente, A. Mai, A. Chiarugi, *Neuroscience* **2018**, *379*, 228-238; cA. Lapucci, L. Cavone, D. Buonvicino, R. Felici, E. Gerace, C. Zwergel, S. Valente, A. Mai, A. Chiarugi, *Neurosci Lett* **2017**, *656*, 120-125; d, PubMed Articles regarding MC1568, p. https://pubmed.ncbi.nlm.nih.gov/?term=MC1568%1520&sort=date&page=1566
[19] A. Mai, S. Massa, S. Valente, S. Simeoni, R. Ragno, P. Bottoni, R. Scatena, G. Brosch, *ChemMedChem* **2006**, *1*, 225-237.
[20] A. Lahm, C. Paolini, M. Pallaoro, M. C. Nardi, P. Jones, P. Neddermann, S. Sambucini, M. J. Bottomley, P. Lo Surdo, A. Carfi, U. Koch, R. De Francesco, C. Steinkuhler, P. Gallinari, *Proc Natl Acad Sci U S A* **2007**, *104*, 17335-17340.
[21] A. Nebbioso, N. Clarke, E. Voltz, E. Germain, C. Ambrosino, P. Bontempo, R. Alvarez, E. M. Schiavone, F. Ferrara, F. Bresciani, A. Weisz, A. R. de Lera, H. Gronemeyer, L. Altucci, *Nat Med* **2005**, *11*, 77-84.
[22] L. Altucci, A. Rossin, W. Raffelsberger, A. Reitmair, C. Chomienne, H. Gronemeyer, *Nat Med* **2001**, *7*, 680-686.

Entry for the Table of Contents

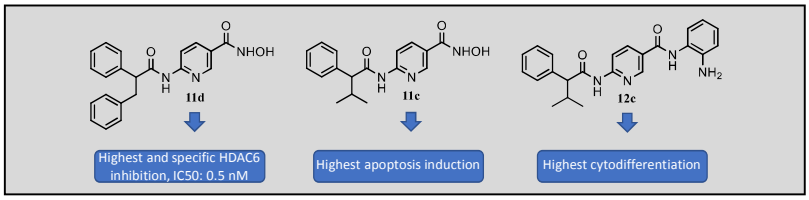

A novel pyridine-based hydroxamates and 2'-aminoanilides as HDAC inhibitors have been described. Among them, the nicotinic hydroxamates, in particular **11d,** proved very high potent inhibition against HDAC6 (IC_{50}: 0.5 nM) with a selectivity index ranging from 100- to 30000-fold over all other HDACs. **11c** displayed the highest apoptosis induction whereas the 2'-aminoanilide **12c** was the best to induce cytodifferentiation in leukemia U937 cells.